

Electronic Supplementary Material (ESI)

Conformational H-bonding Modulations of the Iron Active Site Cysteine Ligand of Superoxide Reductase: Absorption and Resonance Raman Studies.

Alain Desbois,^a Julien Valton,^{‡b} Yohann Moreau,^b Stéphane Torelli,^b and Vincent Nivière^{*b}

^a Institute for Integrative Biology of the Cell (I2BC), CEA, CNRS, Univ Paris-Sud, Université Paris-Saclay, F-91198, Gif-sur-Yvette Cedex, France.

^b Univ. Grenoble Alpes, CNRS, CEA, IRIG-LCBM, F-38000 Grenoble, France. E-mail: vniviere@cea.fr; Tel: (33) 4 38 78 91 09.

[‡] Present address: Celectis, 8 rue de la Croix Jarry, 75013 Paris, France.

Contents: Figures S1, S2, S3, S4 and S5, Tables S1 and S2.

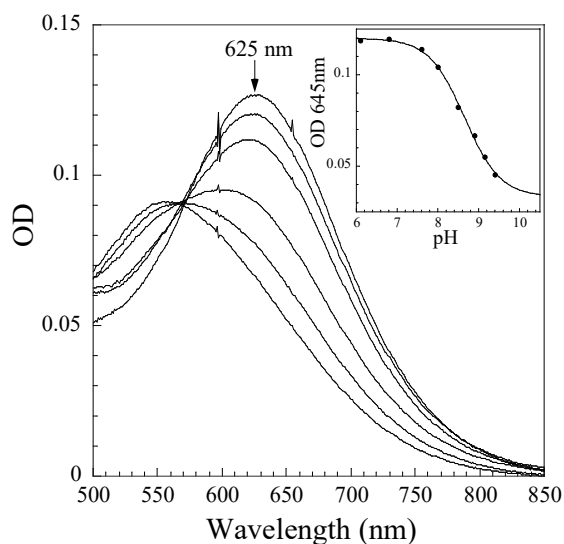


Figure S1. pH-dependence of the electronic absorption spectra of the oxidized active site of the N117A SOR mutant from *D. baarsii*. The enzyme (60 μM in 25 mM of the different buffers) was oxidized with a slight molar excess of K_2IrCl_6 and the spectra were recorded immediately. The spectra, from top to the bottom, at pHs 6.10, 7.60, 8.00, 8.50, 8.90, 9.15 were corrected for the absorbance associated with the Dx iron center. The inset shows the pH-dependence of the absorbance at 645 nm. The titration curve fitted the equation expected from a single protonation process: $A_{645\text{nm}} = (A_{645\text{max}} + A_{645\text{min}} \times 10^{(\text{pH} - \text{pK}_a \text{ app})}) / (1 + 10^{(\text{pH} - \text{pK}_a \text{ app})})$. An apparent pK_a value of 8.65 ± 0.05 was determined. Since the N117A mutant is unstable at pH values higher than 9.2, the absorbance band maximum at alkaline pH could not be determined, but in any case was below 580 nm.

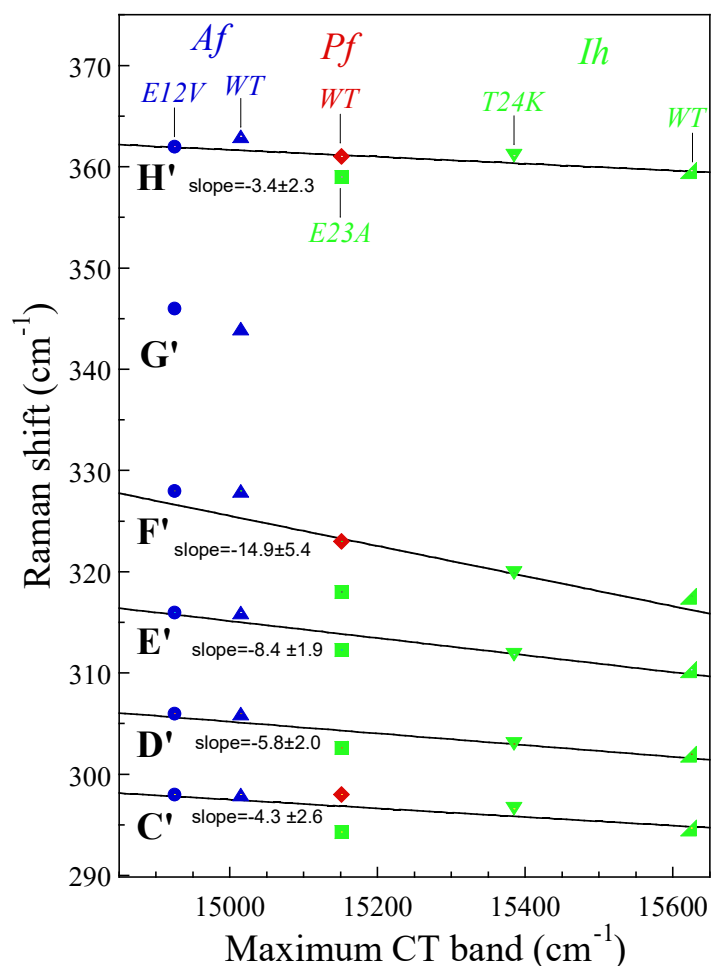


Figure S2. Class II 1Fe-SORs. Plot of the $\nu(\text{Fe-S})$ -involving modes frequencies (290-370 cm^{-1}) vs the maximum of the $(\text{Cys})\text{S}^- \rightarrow \text{Fe}^{3+}$ charge-transfer (CT) band reported for different 1Fe-Class II SORs at neutral or acidic pHs. In blue, RR frequencies and CT band positions of the *Archaeoglobus fulgidus* (*Af*) compounds¹ (WT (▲) and its E12V mutant(●)); in red: RR frequencies and CT band position of the *Pyrococcus furiosus* (*Pf*) WT SOR² (◆); in green: RR frequencies and CT band positions of the *Ignicoccus hospitalis* (*Ih*) compounds,³ WT (▲) and its E23A (■) and T24K (▼) mutants (Table S2). The solid lines correspond to a linear fit calculated for each set of bands. For each set of bands (C'–H'), the slopes are expressed in terms of Raman shifts (cm^{-1}) for a CT variation of 1000 cm^{-1} (Table S2).

Low-frequency RR bands of Class II 1Fe-SORs

The 290-370 cm^{-1} region of the RR spectra of Class-II SORs displays six bands (bands C' \rightarrow H', Fig. S2), homologous in terms of frequency ranges to bands C \rightarrow H of Class I-III SORs (Fig. 4, Table 1). The correlations between the RR frequencies and the CT energies of Class II SORs differ from those of the Class I-III SORs (Figs. 4 and S2). Thus, the different RR profiles shown in Figures 4 and S2 represent two types of RR fingerprints associated to symmetry differences of the catalytic site of Class I-III and Class II SORs.

The most prominent RR band of the *Af* and *Ih* SOR compounds (294-297 cm^{-1} and 298-300 cm^{-1} , respectively) was assigned to a mode carrying the highest Fe-S(Cys) stretching character.^{1,3} This band C' is homolog in frequency to band C of the Class I and Class III SORs (Table 1). However, Figure S2 and

Table S2 show that the slope of the RR frequency/CT energy relationship of band C' are rather modest (-4.3 ± 2.6) when compared to those of band C (-16.0 ± 1.5 , Table 1). Thus, although intense, band C' cannot be assigned to a predominant $\nu(\text{Fe-S}(\text{Cys}))$ stretch like band C of the Class-I and -III SORs (Table 1). Considering its higher slope value (-14.9 ± 5.4 , Table S2), band F' ($316\text{-}329\text{ cm}^{-1}$) appears to be the most appropriate candidate for such an assignment (Fig. S2 and Table S2). Furthermore, it is important to consider that this linear correlation includes the 323 cm^{-1} line of the Pf SOR, which was assigned to a major Fe-S(Cys) stretch on the basis of ^{34}S - and ^{54}Fe - shifts (-3.3 and $+1.1\text{ cm}^{-1}$, respectively).² Although not necessarily the most intense band of the RR spectra, all these data converge toward a primarily $\nu(\text{Fe-S}(\text{Cys}))$ motion for band F' of the Af-, Ih- and Pf- SORs.

Thus, for a same energy level in CT transition, the Fe-S(Cys) bond of the Class-II SORs is therefore stronger than that of the Class I or Class III SORs (Tables 1 and S2). For a same CT energy, the strength of the trans Fe-O(Glu) bond is thus expected to be weaker in the Class II SORs.

Like for the couples of bands C'/C and F'/F, the slope of bands D' (-5.8 ± 2.0) and H' (-3.4 ± 2.3) of the Class II SORs (Fig. S2 and Table S2) differs significantly from that of their homologous bands D (-17.9 ± 1.6) and H (~ 0) of the Class I-III SORs (Table 1). In addition to differences in Fe-S bond strength and PED contribution, these different behaviors indicate large variations in the coupling of the Fe-S(Cys) mode with Fe-S-C $_{\beta}$ -C $_{\alpha}$ deformation modes. Considering the axial symmetry of the active site of Class-II SORs,⁴ a RR activity of an antisymmetric mode involving major $\nu(\text{Fe-S}(\text{Cys}))$ stretch is not allowed.

Different structural levels could determine the Class-specific RR fingerprints of SORs. As far as the tertiary structures are concerned, the catalytic domain in each Class of SORs adopts a similar architecture with a 3 + 4 stranded β -barrel in an immunoglobulin-like fold. However, obvious differences between Class-II SORs and both Class I and III SORs are that the later have five shorter β -strands (from $\beta 3$ to $\beta 7$) and a shorter $\beta 3 \rightarrow \beta 4$ loop around the active site.^{5,6} Thus, changes in oxidation state of the metal atom coupled with the coordination state of the Glu ligand produce modifications in length of β -strands and loops. In addition, in all the available X-ray structures, the Cys ligand occupies the C-terminal end of the $\beta 6$ -strand, which has a variable size: 6 residues for the Class I and 9 for Class II SORs. The length of the $\beta 7$ -strand is also Class-specific with 5-6 residues for the Class I and III SORs and 8-11 residues for the Class III SORs. These differences in β -strand length as well as in loop length could induce variations in local protein rigidity and folding of the loops, which could have impacts into the Fe³⁺ coordination sphere.

Therefore, the coordination state of the Class I and Class III SORs seems to be more strained than that of Class II SORs, locked by six amino-acid ligands belonging to well-structured peptide regions. This less strained state may be at the origin of a decreased distortion of the iron coordination in the Class II SORs.

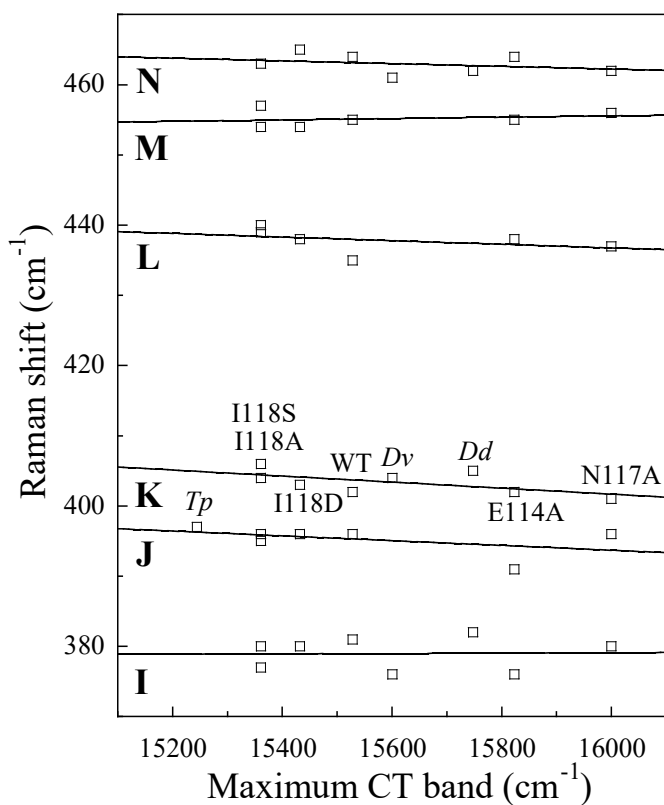


Figure S3. Plot of the RR frequencies of modes of the 370-470 cm^{-1} region vs the maximum of the $(\text{Cys})\text{S}^- \rightarrow \text{Fe}^{3+}$ CT absorption bands reported at neutral pHs for SORs from *D. baarsii*, WT and mutants N117A, I118D, I118S, I118A, E114A (Table 1); from *Desulfovibrio vulgaris* (*Dv*), *Desulfovibrio desulfuricans* (*Dd*) and *Treponema pallidum* (*Tp*). The plot shows RR bands I, J, K, L, M and N listed in Table 1. The solid lines correspond to a linear fit calculated for each set of bands (Table 1).

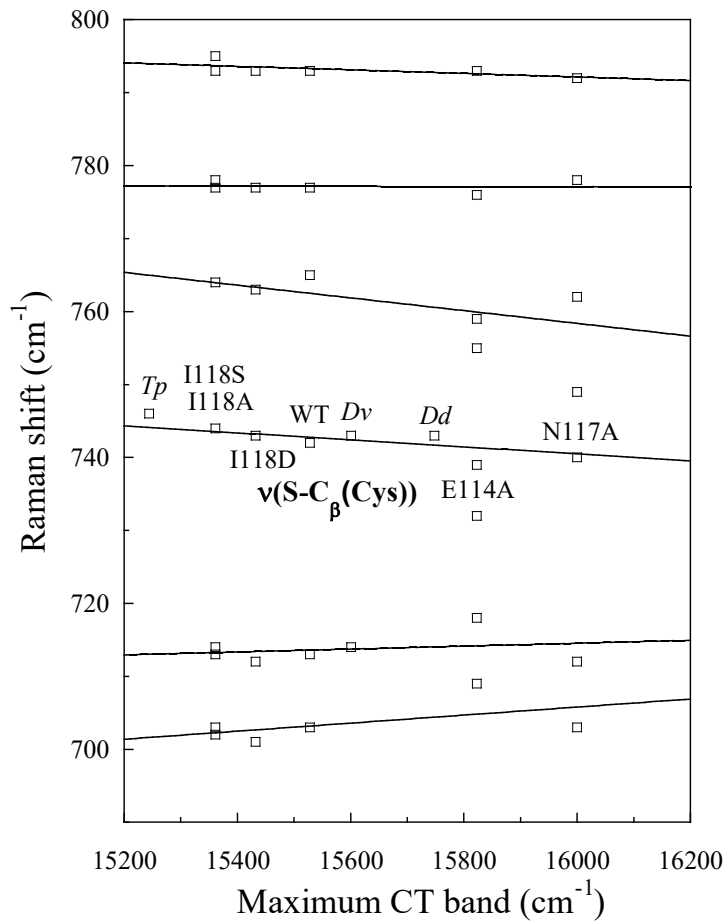


Figure S4. Plot of the frequencies of the RR bands of the 700-800 cm⁻¹ region versus the maximum of the (Cys)S⁻ → Fe³⁺ charge-transfer (CT) bands reported at neutral pHs for SORs from *D. baarsii*, WT and mutants N117A, I118D, I118S, I118A, E114A (Table 1); from *Desulfovibrio vulgaris* (*Dv*), *Desulfovibrio desulfuricans* (*Dd*) and *Treponema pallidum* (*Tp*). The solid lines correspond to a linear fit calculated for each set of bands (Table 1).

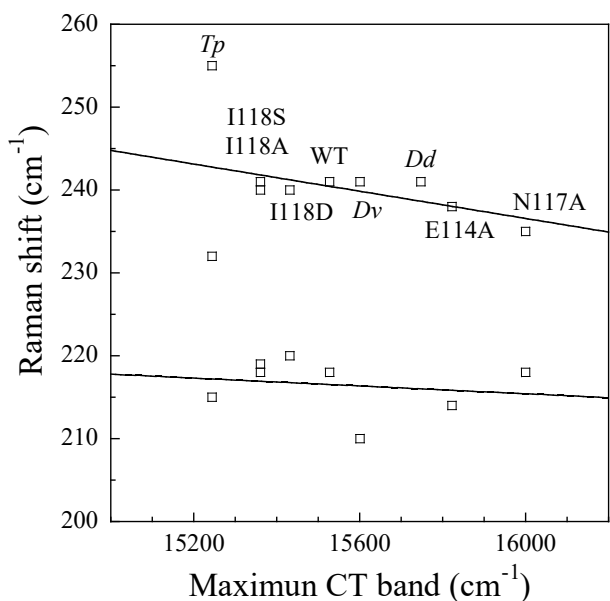


Figure S5. Plot of the frequencies of the RR bands of the 200-260 cm^{-1} region versus the maximum of the $(\text{Cys})\text{S}^- \rightarrow \text{Fe}^{3+}$ charge-transfer (CT) bands reported at neutral pHs for SORs from *D. baarsii*, WT and mutants N117A, I118D, I118S, I118A, E114A (Table 1); from *Desulfovibrio vulgaris* (*Dv*), *Desulfovibrio desulfuricans* (*Dd*) and *Treponema pallidum* (*Tp*). The solid lines correspond to a linear fit calculated for each set of bands (Table 1).

Table S1. Frequencies (cm^{-1}), relative intensities (I_N), frequency shifts ($\Delta\nu$ in cm^{-1}), intensity ratios of the bands of the 270-370 cm^{-1} region of the RR spectra of the *D. baarsii* SOR WT and N117A mutant (see also Figure 3).

Band	WT		N117A		$\Delta\nu$ (N117A - WT)	$I_{N(\text{N117A})}/I_{N(\text{WT})}$
	ν	I_N	ν	I_N		
A	277.1	0.137	276.6	0.154	-0.5	1.12
B	287.1	0.344	284.7	0.667	-2.4	1.94
C	298.9	1	293.1	1	-5.8	1
D	305.7	0.222	298.1	0.521	-7.6	2.35
E	316.9	0.967	310.8	0.416	-6.1	0.43
F	324.1	0.235	316.8	1.084	-7.3	4.61
	332.7	0.114				
G	344.5	0.098	340.7	0.258	-3.8	2.63
H	357.6	0.703	356.4	0.293	-1.2	0.42

Table S2. Observed frequencies of the RR bands of oxidized Class II SORs from *Archaeoglobus fulgidus* (Af), WT and E12V mutant, *Pyrococcus furiosus* (Pf) WT and *Ignicoccus hospitalis* (Ih) WT, T24K and E23A mutants.

Band	Af WT ^a	Af E12V ^a	Pf WT ^b	Ih WT ^c	Ih T24K ^c	Ih E23A ^c	slope ^d	Assignment
C'	298 -	- 298	298 "	294.7 "	296.6 "	- 294.3	-4.3 ± 2.6	
D'	306 -	- 306		302 "	303 "	- 302.6	-5.8 ± 2.0	
E'	316 "	- 316		310.3 "	311.8 "	- 312.3	-8.4 ± 1.9	$\delta(\text{SC}_\beta\text{C}_\alpha) + \nu(\text{FeS}(\text{Cys}))$
F'	328 "	- 328	323 "	317.6 "	319.9 "	- 318	-14.9 ± 5.4	$\nu(\text{FeS}(\text{Cys})) + \delta(\text{Cys})$
G'	344 "	- 346						
H'	363 "	- 362	361 "	359.6 "	361.1 "	- 359	-3.4 ± 2.3	

^a From reference ¹.

^b From reference ².

^c From reference ³.

^d Slope values, calculated from Fig. S2, are expressed in term of Raman shifts (cm⁻¹) for a CT band variation of 1000 cm⁻¹.

References

- 1 S. Todorovic, J. V. Rodrigues, A. F. Pinto, C. Thomsen, P. Hildebrandt, M. Teixeira and D. H. Murgida, *Phys. Chem. Chem. Phys. PCCP*, 2009, **11**, 1809–1815.
- 2 M. D. Clay, F. E. Jenney, H. J. Noh, P. L. Hagedoorn, M. W. W. Adams and M. K. Johnson, *Biochemistry*, 2002, **41**, 9833–9841.
- 3 A. F. Pinto, C. V. Romão, L. C. Pinto, H. Huber, L. M. Saraiva, S. Todorovic, D. Cabelli and M. Teixeira, *J. Biol. Inorg. Chem. JBIC Publ. Soc. Biol. Inorg. Chem.*, 2015, **20**, 155–164.
- 4 M. D. Clay, F. E. Jenney, P. L. Hagedoorn, G. N. George, M. W. W. Adams and M. K. Johnson, *J. Am. Chem. Soc.*, 2002, **124**, 788–805.
- 5 A. V. Coelho, P. Matias, V. Fülöp, A. Thompson, A. Gonzalez and M. A. Carrondo, *JBIC J. Biol. Inorg. Chem.*, 1997, **2**, 680–689.
- 6 A. P. Yeh, Y. Hu, F. E. Jenney, M. W. Adams and D. C. Rees, *Biochemistry*, 2000, **39**, 2499–2508.